

EUROPEAN ORGANIZATION FOR NUCLEAR RESEARCH

CERN-PPE/94-70

May 4th, 1994

# PRECISION STUDIES OF ELECTROWEAK INTERACTIONS AT LEP<sup>1</sup>

Ramon MIQUEL  
CERN, PPE Division  
CH-1211 Geneva 23  
Switzerland

**Abstract:** The results on electroweak interactions obtained at LEP during 1989–1993 are reviewed and compared with the Minimal Standard Model predictions. The overall agreement is good and allows for an indirect determination of the top quark mass:  $m_t = (165_{-14}^{+13+18})$  GeV, where the second error reflects the uncertainty in the Higgs boson mass.

## 1 Introduction

Testing the theory of the electroweak interactions, the Minimal Standard Model (MSM), has been one of the main activities of LEP since its start-up in 1989. Every electroweak observable  $O_i$  can be computed in the MSM as a function of the parameters that define the theory

$$O_i = f_i(\alpha, G_\mu, M_Z, m_f, M_H, \alpha_s). \quad (1)$$

The first three parameters are known very precisely:  $\alpha$ , the fine structure constant, to better than  $10^{-7}$ ;  $G_\mu$ , the muon decay constant, to  $2 \cdot 10^{-5}$ ; and  $M_Z$ , the Z mass (measured at LEP), to  $5 \cdot 10^{-5}$ . The fermion masses,  $m_f$ , are also well known, except for the mass of the top quark,  $m_t$ , not yet discovered. The Higgs boson mass,  $M_H$ , is totally unknown. As for the strong coupling constant at the Z scale,  $\alpha_s(M_Z^2)$ , which appears in any weak process involving quarks, is known to about 5%

---

<sup>1</sup>Talk presented at the 22nd INS Symposium: “Physics with High Energy Colliders”, Tokyo (Japan), March 8–10, 1994.

The goal of the electroweak measurements at LEP is both to get information on the least known parameters of the theory,  $m_t$ ,  $M_H$  and  $\alpha_s$ , and to test the overall structure of the MSM, irrespectively of the values of its parameters. To achieve this goal, the strategy is simple: as many observables  $O_i$  as possible are measured as accurately as possible and then are confronted with the predictions of the Minimal Standard Model as a function of  $m_t$ ,  $M_H$  and  $\alpha_s$ . One obtains then best fit values for these parameters and, from the overall quality of the fit, a test of the theory.

The results presented here come, for most observables, from all data taken between 1989 and 1993 by the four LEP experiments: almost two million hadronic Z decays and about two-hundred thousand charged-lepton Z decays per experiment. Most of the results are still preliminary. Ref. [1] contains a detailed explanation of the procedure used to combine the 1992 data. A similar report is in preparation with the 1993 data.

The observables presented are divided into three groups: the lineshape parameters, which parametrize the leptonic and hadronic cross section measurements; the partial width of the Z to b quarks; and the so-called asymmetries which measure the effective weak mixing angle,  $\sin^2 \theta_W^{eff}$ . They are discussed in turn in the following.

## 2 Lineshape parameters

The cross section for the production of a fermion pair  $f\bar{f}$  is written as

$$\sigma_{f\bar{f}}(s) = \int_{4m_f^2}^s ds' H(s, s') \hat{\sigma}_{f\bar{f}}(s') \quad (2)$$

where  $H(s, s')$  is the so-called radiator function which takes care of initial state radiation corrections and the reduced cross section  $\hat{\sigma}$  is written as

$$\hat{\sigma}_{f\bar{f}}(s) = \sigma_{f\bar{f}}^0 \cdot \frac{s\Gamma_Z^2}{(s - M_Z^2)^2 + \left(\frac{s\Gamma_Z}{M_Z}\right)^2} + (\gamma - Z) + |\gamma|^2 \quad (3)$$

where the two last terms are taken from theory. This parametrization assumes the validity of QED for the photon exchange part and also takes from the Minimal Standard Model the interference between the photon- and Z-mediated amplitudes. This interference is very small around the Z pole. In the case of Bhabha scattering,  $f = e$ , one has to add the t-channel photon- and Z-exchange diagrams, also taken from the theory. The cross section at the peak can be written in turn in terms of the Z mass and width and the Z partial widths to the initial state  $\Gamma_e$  and the final state  $\Gamma_f$ :

$$\sigma_{f\bar{f}}^0 = \frac{12\pi}{M_Z^2} \cdot \frac{\Gamma_e \Gamma_f}{\Gamma_Z^2} \quad (4)$$

Assuming lepton universality, four parameters are needed to describe the s-dependence of the hadronic and leptonic cross sections: the Z mass ( $M_Z$ ) and total width ( $\Gamma_Z$ ), the ratio

of hadronic to leptonic partial widths ( $R_l = \Gamma_h/\Gamma_l$ ) and the hadronic peak cross section ( $\sigma_h^0$ ). If lepton universality is not assumed,  $R_l$  is substituted by three analogous quantities,  $R_e$ ,  $R_\mu$ ,  $R_\tau$ .

Two computer programs which implement the scheme sketched above have become the standard ones at LEP: MIZA [2] is used by the ALEPH collaboration; ZFITTER [3] by DELPHI, L3 and OPAL. At the current level of experimental precision, the results obtained with both of them are equivalent.

Since in 1993 an energy scan around the Z resonance was performed, the precision in the measurement of the lineshape parameters has been greatly improved with respect to the previous year.

## 2.1 Z mass

The Z mass is the most precise single measurement performed at LEP. The results by the four experiments are shown in fig. 1. The main error is a common uncertainty of  $\pm 0.004$  GeV due to the limited knowledge of the absolute energy scale of the machine [4]. The method used to measure the beam energy is based on resonant depolarization by an oscillating magnetic field. The intrinsic precision is a fraction of an MeV but the bulk of the error comes from remaining uncertainties in the stability of the energy, which is affected by the status of the radiofrequency cavities, the temperature and humidity in the LEP tunnel and the tidal forces of the sun and the moon, which change the circumference of the machine by as much as 1 mm, affecting the beam energy at the few MeV level [5] (fig. 2).

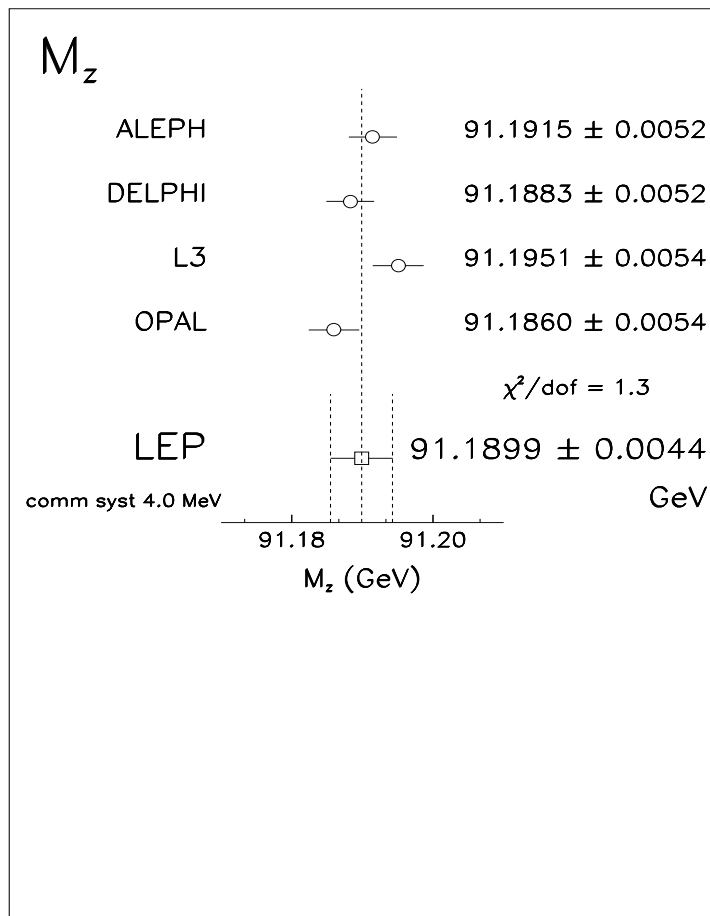
The error given above is a preliminary estimate and can probably be improved through more studies by the LEP energy group. In particular, there is a suspicion that a seasonal effect, maybe related to the water content in the soil around LEP, produces a variation with time of the radius of the ring and, hence, the energy. This would explain a certain scattering in the measurements of the energy which for the moment is not fully understood. A final error below 3 MeV seems feasible.

## 2.2 Z width

The Z width is a very useful observable because of its strong dependence on the top quark mass. Fig. 3 shows the LEP results together with the MSM prediction as a function of  $m_t$ . As in the case of the Z mass, the main error comes from the accelerator: in this case from the knowledge of the difference in LEP energy between two scan points. During 1993 the resonant depolarization technique was used in the three scan points and this has brought this error down to 2.7 MeV [4]. As in the previous case, there is hope to reduce it further down to 2 MeV or less with more studies.

The other important source of uncertainty here is the precise knowledge of the background from non-resonanting processes like quasi-real photon-photon collisions. The current error is close to 2 MeV per experiment but incoherent among them. The theoretical error associated with the extraction and interpretation of the width measurement is at the moment thought to be small, below 1 MeV.

Figure 1: The Z mass measured by the four experiments together with the mean. The numerical values given include the errors common to the four experiments, while the error bars for the four experiments do not, to give a visual impression of the agreement between them, which can also be seen from the value of  $\chi^2$  per degree of freedom.

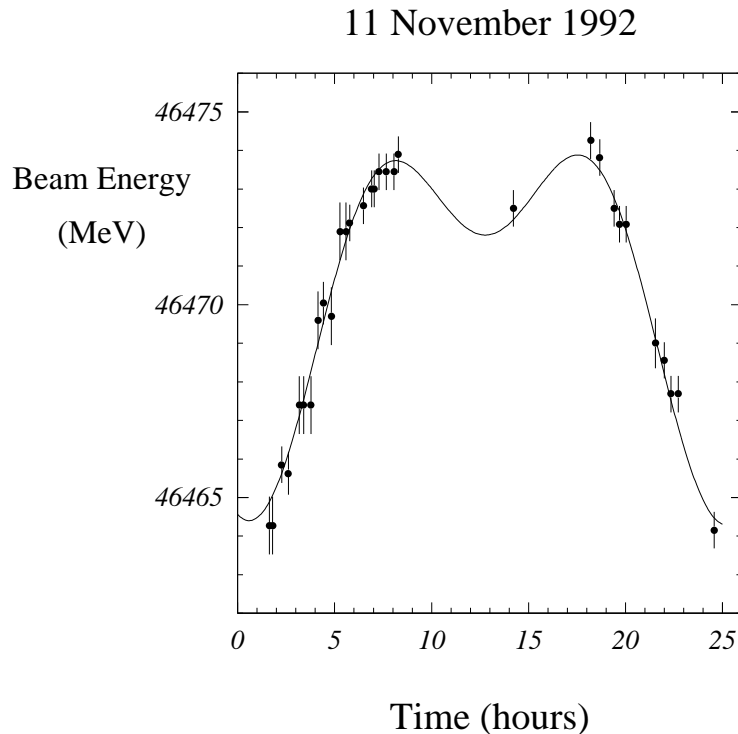


### 2.3 $R_l = \Gamma_h/\Gamma_l$

The results of the measurements of  $R_l$ , the ratio of the hadronic to the leptonic Z partial widths are given in fig. 4. It should be noted that the result is given for a massless lepton. The mass correction is only non-negligible for the tau lepton, given the current precision.

The experimental systematic error is dominated by the knowledge of the efficiencies and backgrounds in the leptonic channels: about 0.5% per experiment. On top of this, there is a common error coming from the t-channel correction in the electron channel, which contributes 0.1% to the error in  $R_l$ . This uncertainty is directly due to the lack of a full  $\mathcal{O}(\alpha^2)$  Monte Carlo event generator for Bhabha scattering.

Figure 2: Effect of the tidal forces of the moon and the sun on the LEP energy. The dots represent the energy measured with resonant depolarization, while the solid line is the prediction.



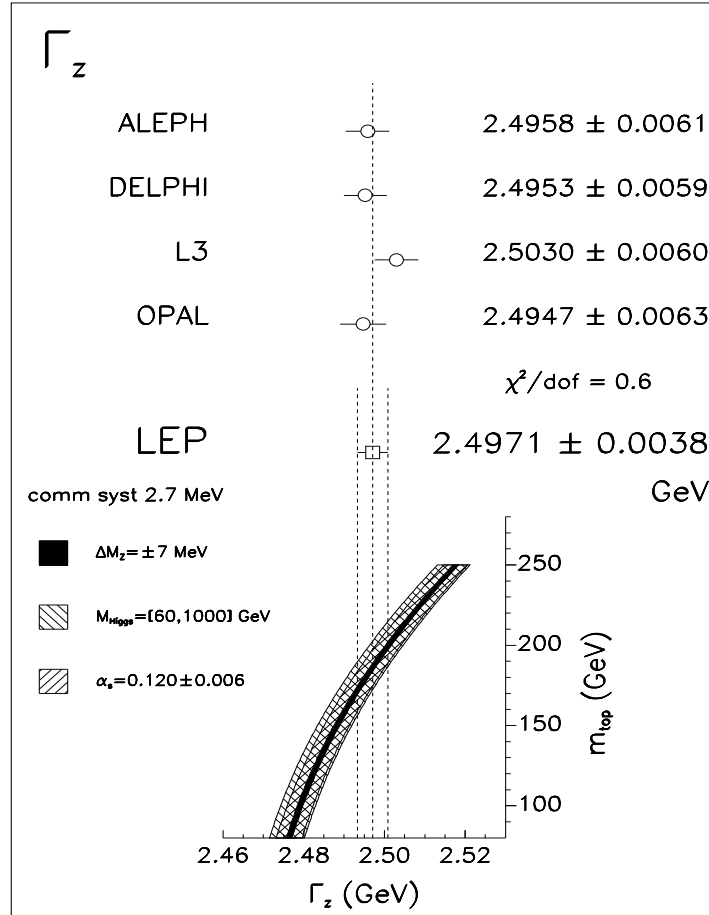
As can be seen from fig. 4,  $R_l$  is not very dependent either on  $m_t$  or on  $M_H$ . However, its dependence on the strong coupling constant makes it an ideal variable to determine  $\alpha_s(M_Z^2)$  with minimum theoretical uncertainties. To do so, one has to assume the validity of the MSM, but it should be pointed out that extensions of the MSM which would manifest themselves mainly via effects in vacuum polarization would not show up in  $R_l$ , being a ratio of widths, exactly for the same reason as why the  $m_t$  dependence is so small.

Using the mean value of  $R_l$  and the formulas of [6], which relate  $R_l$  with the QCD prediction, known to  $\mathcal{O}(\alpha_s^3)$ , one gets

$$\begin{aligned} \alpha_s(M_Z^2) &= 0.124 \pm 0.006 \pm 0.002_{ew} \pm 0.002_{QCD} \pm 0.003_{m_t, M_H} \\ &= 0.124 \pm 0.007 \end{aligned} \quad (5)$$

where the second and third error reflect uncertainties on the electroweak and QCD parts of the theoretical prediction respectively, and the last one comes from the lack of knowledge on the top quark and Higgs masses.

Figure 3: The  $Z$  width measured by the four experiments together with the mean and the MSM prediction as a function of the top quark mass. The error definitions are those of fig. 1.

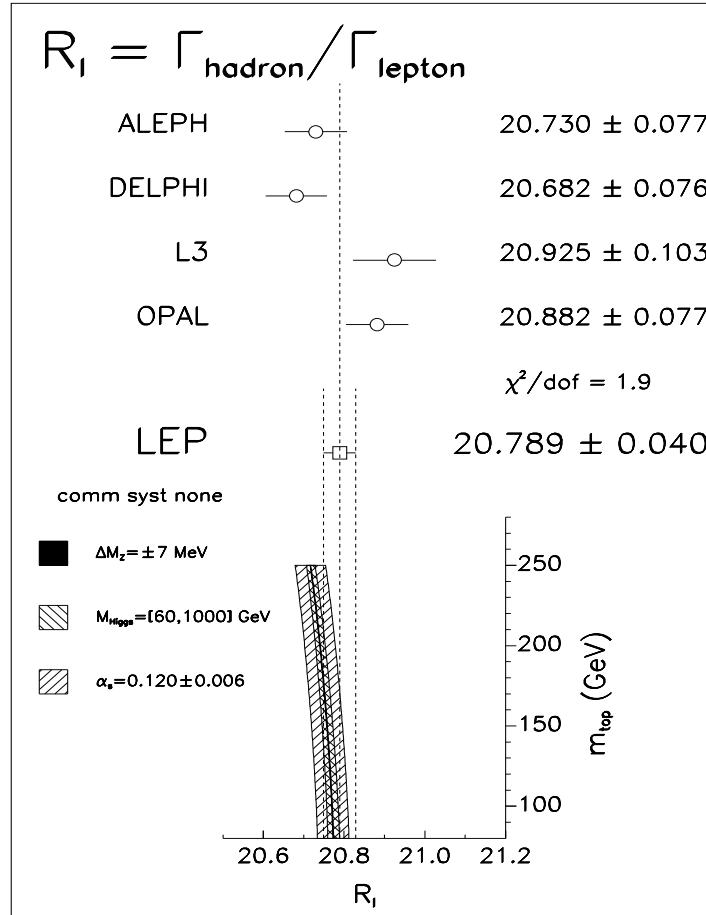


## 2.4 Hadronic peak cross section

The measurements by the four collaborations of the hadronic peak cross section,  $\sigma_h^0$ , are shown in fig. 5. There are three main contributions to the error:

- The knowledge of the efficiency and background of the hadron selection contributes about 0.2% per experiment, uncorrelated, and it can probably be improved.
- The experimental uncertainty in the measurement of the absolute luminosity is very different depending on the experiment, although all of them have recently upgraded their luminosity set-ups and will probably reach an error between 0.1% and 0.2% when the analysis are finalized.

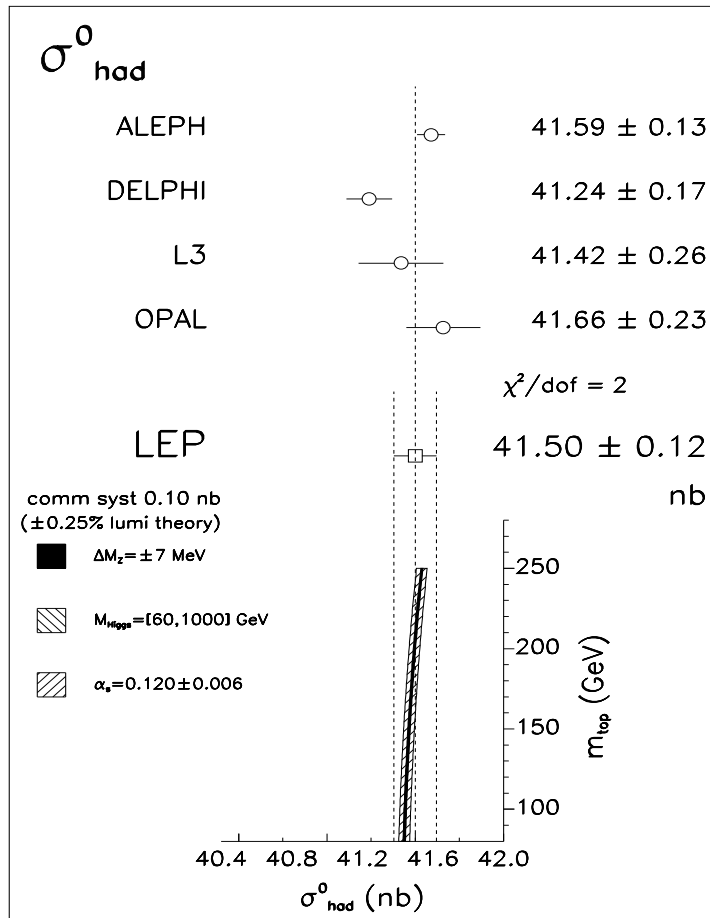
Figure 4: The ratio of hadronic to leptonic Z partial widths measured by the four experiments together with the mean and the MSM prediction as a function of the top quark mass. The error definitions are those of fig. 1.



- The theoretical error in the low-angle Bhabha cross section (currently estimated as 0.25%) is the largest uncertainty and is common for the four experiments. There is, however, hope to improve it to around 0.1% through the work of, at least, two groups of theoreticians [7, 8].

The Minimal Standard Model prediction, also shown in fig. 5, is not very sensitive to the top quark or Higgs masses nor to the strong coupling constant. Therefore, the hadronic peak cross section is an ideal variable to test for possible deviations from the MSM without the uncertainty related to the lack of knowledge in some of its parameters. For example, limits on the mixing angle between the Z boson and a hypothetical extra heavy neutral boson, Z', around 0.005 can be obtained using only  $\sigma_h^0$ ,  $M_Z$  and a measurement of  $\alpha_S$  from jet studies.

Figure 5: The hadronic peak cross section measured by the four experiments together with the mean and the MSM prediction as a function of the top quark mass. The error definitions are those of fig. 1.



## 2.5 Derived quantities

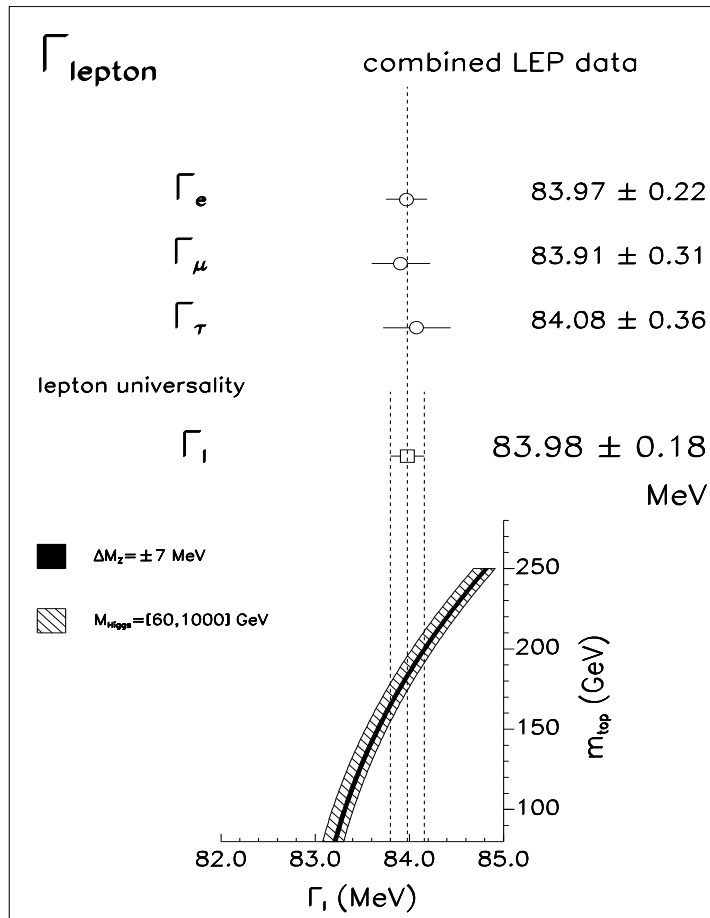
The four quantities described in the previous section are enough to describe all the lineshape data, assuming lepton universality. From them one can get the rest of the  $Z$  parameters using  $\Gamma_Z = \Gamma_h + \Gamma_e + \Gamma_\mu + \Gamma_\tau + \Gamma_{inv}$  and equation 4.

A check of lepton universality can be obtained by comparing the three charged lepton partial widths, as shown in fig. 6. The three results agree well and the mean value (corrected to represent that of a massless lepton) is interesting to constrain the top mass, because it does not depend on  $\alpha_s$ , while  $\Gamma_Z$  does.

The number of light neutrino families is obtained from the ratio of the invisible width,



Figure 6: The partial widths measured at LEP for the three charged leptons, the combined result corrected to a massless lepton and the MSM prediction as a function of the top quark mass.

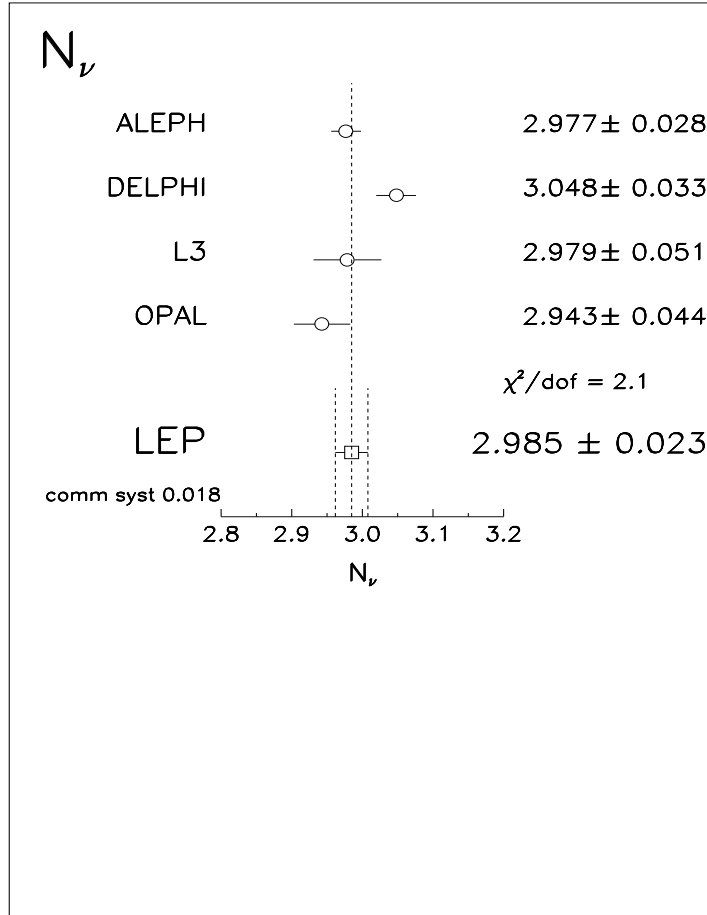


$\Gamma_{inv}$ , to the leptonic width. One has to assume that all the invisible width is due to neutrino final states, write

$$\frac{\Gamma_{inv}}{\Gamma_l} = N_\nu \cdot \frac{\Gamma_\nu}{\Gamma_l} \quad (6)$$

and take the ratio  $\Gamma_\nu$  over  $\Gamma_l$  from the MSM:  $\Gamma_\nu/\Gamma_l = 1.992 \pm 0.003$ . It should be noted the small error in the Minimal Standard Model prediction for this ratio, which does not depend on  $\alpha_s$  and in which the top and Higgs mass dependences largely cancel. Fig. 7 shows the results of the four collaborations. Since the result favours three species without any doubt, this measurement is actually a test of the MSM, a test of the assumptions made: that all invisible decays are to neutrinos, and of the value  $\Gamma_\nu/\Gamma_l$ . If  $N_\nu = 3$  is assumed, the

Figure 7: The number of light neutrino families measured by the four experiments together with the mean. The error definitions are those of fig. 1.



measurement of  $N_\nu$  can be turned into a measurement of  $\Gamma_\nu/\Gamma_l$ :

$$\frac{\Gamma_\nu}{\Gamma_l} = 1.983 \pm 0.015 . \quad (7)$$

This quantity can also be used to put limits on the mixing of extra neutral bosons to the Z, if one wants to avoid using external information on the strong coupling constant.

### 3 $R_b = \Gamma_b/\Gamma_h$

The measurement of the Z decay width into b hadrons is especially important because, within the Minimal Standard Model, it receives a radiative correction involving the top quark which

is absent from any other final state, due to the smallness of the relevant elements of the Cabbibo-Kobayashi-Maskawa matrix. This is an independent source of information on the top mass but also on new physics: extensions of the Minimal Standard Model which would not contribute to vacuum polarization corrections could contribute to this vertex correction.

By taking the ratio of  $\Gamma_b$  to  $\Gamma_h$ , most of the vacuum polarization corrections depending on the top quark and the Higgs mass cancel out, and one is left with the following approximate expression:

$$R_b \simeq R_d \cdot \left[ 1 - \frac{20}{13} \frac{\alpha}{\pi} \left( \frac{m_t^2}{M_Z^2} + \frac{13}{6} \log \frac{m_t^2}{M_Z^2} \right) \right] \quad (8)$$

This ratio is also insensitive to extensions of the MSM which would only contribute to vacuum polarizations.

The whole effect of the top quark corrections is only of order 2% for a top mass of 150 GeV. This means that only a precise measurement, to better than 1%, is useful to get information on the top mass. With the new preliminary measurements just made available by the LEP collaborations the overall error has reached a very interesting 0.9%

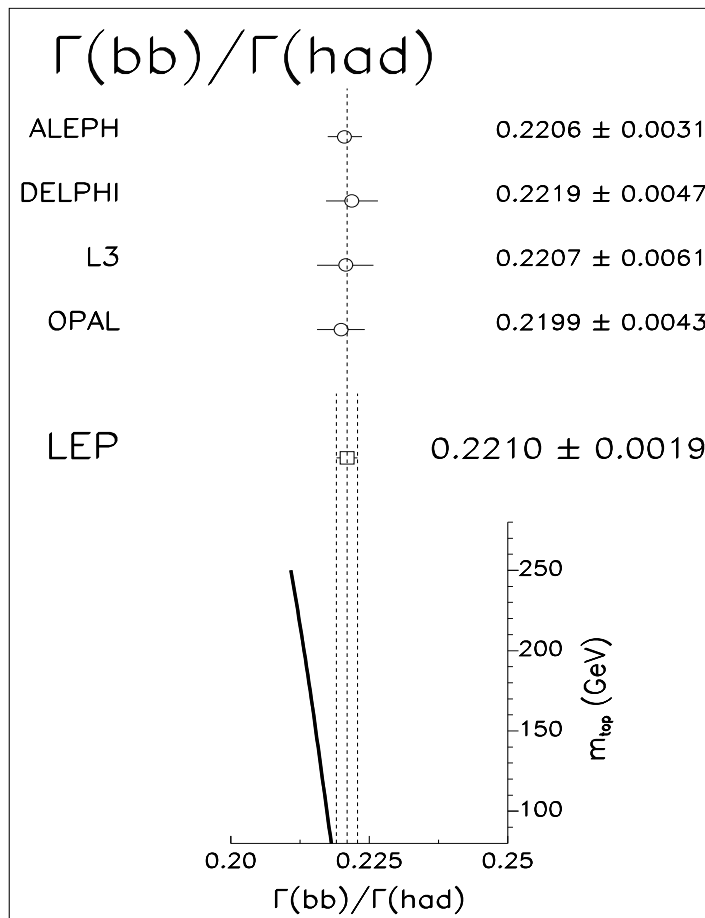
Based on three distinguishing properties of the b quark, three methods have been used to identify b events at LEP:

- Lepton tag: It uses high  $p$ , high  $p_t$  leptons from b decays. High purity can be achieved but one has to pay for the small semileptonic b branching ratio.
- Event shape tag: High mass, high momentum b mesons or baryons give raise to particular event shapes which have been used to tag b events with high efficiency although rather modest purity.
- Lifetime tag: The long lifetime of the b quark can be used, using silicon microvertex detectors, to tag b events by looking for tracks not coming from the Z production vertex. This is currently the best performing method with both high purity and efficiency.

The main systematic errors come from the evaluation of the efficiency and the background of the selection. The best option is to try to use data to estimate both. In the case of the efficiency, the techniques mentioned above can be used to tag only one hemisphere and look at the other one to measure the tag efficiency. Similar techniques could also be used for the backgrounds.

The results from the four collaborations are shown in fig. 8. The agreement between them is excellent but not the one with the MSM, which predicts a quite lower number. The current central value of the mean corresponds to a negative value for  $m_t^2$  and is more than two standard deviations away from values of  $m_t$  above 150 GeV, as favoured by the other electroweak measurements. Some extensions of the MSM would give raise to such an enhancement. Among them, the minimal supersymmetric extension of the MSM in the case of light charginos. However, at present, it can be explained by a statistical fluctuation. And there is also the worry of some effects like events where a gluon splits into a  $b\bar{b}$  pair while the Z decays to some other quark pair, which might have been improperly estimated.

Figure 8: The ratio of the Z partial widths to b hadrons to the one to all hadrons measured by the four experiments together with the mean and the MSM prediction as a function of the top quark mass. The error definitions are those of fig. 1.



## 4 Asymmetries

The measurement of the effective weak mixing angle,  $\sin^2 \theta_W^{eff}$ , is of paramount importance. It allows for an indirect determination of the top quark mass and gives also some (small) information on the Higgs boson, apart from being sensitive to new physics. The angle is defined via the ratio of the effective vector and axial vector fermion couplings to the Z:

$$\sin^2 \theta_W^{eff} = \frac{1}{4} \left( 1 - \frac{g_v^f}{g_a^f} \right) \quad (9)$$

To be precise, the angle presented in the following is defined via the ratio of the charged lepton couplings: the angle determined from quark final states is (slightly) corrected to this

definition.

The quantities which measure these ratios of vector to axial-vector couplings are usually known as asymmetries and are discussed in the following.

## 4.1 Lepton Forward-Backward Asymmetry

The leptonic forward-backward asymmetry can be defined as

$$A_{FB}^l = \frac{\sigma_F - \sigma_B}{\sigma_F + \sigma_B}, \quad (10)$$

where  $F$  and  $B$  indicate whether the positively charged lepton goes into the forward or backward hemisphere. Normally it is measured by fitting the lepton angular distribution to the formula

$$\frac{d\sigma^l}{d\cos\theta}(s) = \frac{3}{8}\sigma^l(s) \cdot \left(1 + \cos^2\theta + \frac{8}{3}A_{FB}^l(s)\cos\theta\right). \quad (11)$$

In the case of  $e^+e^-$  final state, the t-channel contribution has to be added.

Once the different  $A_{FB}^l(s_i)$  are obtained, they are fitted together with the lineshape data to get the the lineshape parameters mentioned above and the peak asymmetry,  $A_{FB}^{0,l}$ :

$$\begin{aligned} A_{FB}^{0,l} &= \frac{3}{4}A_e A_l \\ A_f &= \frac{2g_v^f/g_a^f}{1 + (g_v^f/g_a^f)^2}. \end{aligned} \quad (12)$$

from which the effective weak mixing angle is measured. The results of the four collaborations are shown in fig. 9. The mean result corresponds to a top quark mass between around 150 and 200 GeV. It can be seen that the agreement between the experiments (and, in particular, between ALEPH and OPAL) is not excellent. The main error is still statistical. Experimental systematics can only come from simultaneous charge and forward-backward asymmetries in the detector, which are bound to be very small. The knowledge of the beam energy contributes a non-negligible 0.0008 to  $\Delta A_{FB}^{0,l}$ , although this can be improved. Theory uncertainties are thought to be considerably smaller.

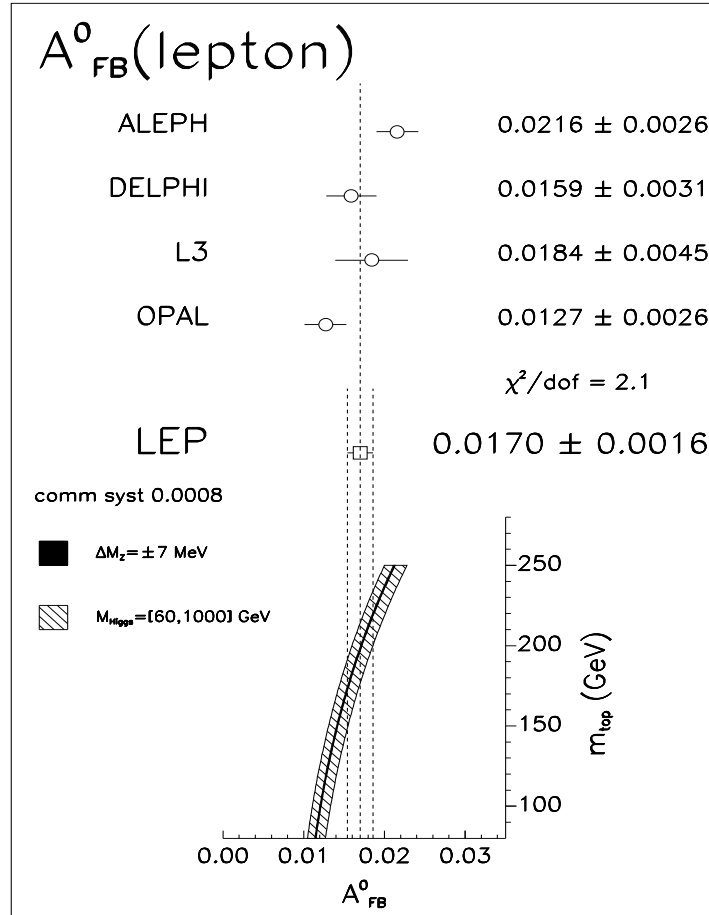
## 4.2 Mean Tau Polarization

The measurement of the mean tau polarization

$$\langle P_\tau \rangle = \frac{\sigma_R - \sigma_L}{\sigma_R + \sigma_L} = -A_\tau, \quad (13)$$

where  $\sigma_{R(L)}$  is the integrated cross section for right (left) handed tau's, provides a means to measure the tau lepton couplings to the Z directly. The tau helicity information is obtained

Figure 9: The leptonic forward-backward asymmetry measured by the four experiments together with the mean and the MSM prediction as a function of the top quark mass. The error definitions are those of fig. 1.



by analysing its decay properties. The main decays are used: to electron, muon, pion, rho, and  $a_1$ . As an example, in the pion channel (which is, together with the rho channel, the most useful) the scaled energy of the pion is measured and the mean tau polarization is extracted from

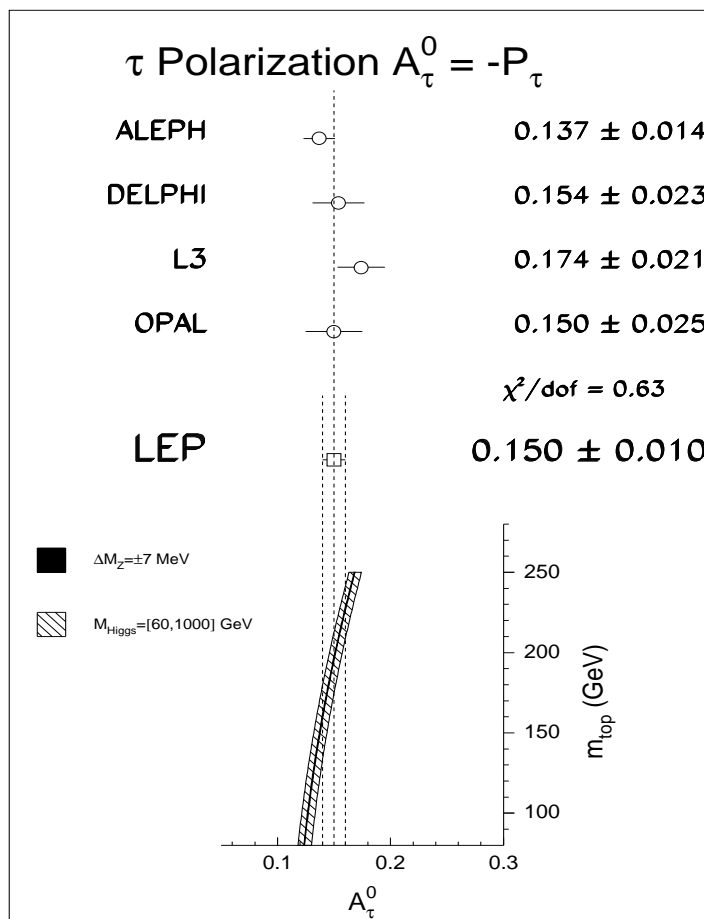
$$\frac{1}{N} \frac{dN}{dx} = 1 + \langle P_\tau \rangle (2x - 1), \quad \text{with}$$

$$x = \frac{E_{\pi^-}}{E_{\text{beam}}} = \frac{1}{2} (1 + \cos \theta^*), \quad (14)$$

$\theta^*$  being the tau decay angle. In the  $\rho$  and  $a_1$  channel, also the  $\rho$  and  $a_1$  decay angles are used.

The results are given in fig. 10 and show good agreement among the experiments and with the MSM prediction with a top mass in the range 150–200 GeV. The systematics are

Figure 10: The mean tau polarization measured by the four experiments together with the mean and the MSM prediction as a function of the top quark mass. The error definitions are those of fig. 1.



in this case as large as the statistical errors. In the  $\pi$  channel they come from the knowledge of both the efficiency as a function of the pion energy and the  $\pi^{-}\pi^0$  background. In the  $\rho$  channel, the main problem is to separate correctly the neutral and charged pions, since the difference of their energies is used to measure the  $\rho$  decay angle. Improvements are certainly possible but not easy. This is a very demanding measurement for the apparatus, especially the calorimeters.

### 4.3 Tau Polarization Forward-Backward Asymmetry

Instead of measuring just the average tau polarization, it can be measured as a function of the tau production angle,  $\theta$ . Then, one gets

$$P_\tau(\cos\theta) = \frac{\frac{d\sigma_R}{d\cos\theta} - \frac{d\sigma_L}{d\cos\theta}}{\frac{d\sigma_R}{d\cos\theta} + \frac{d\sigma_L}{d\cos\theta}} = -\frac{A_\tau + A_e \cdot \frac{2\cos\theta}{1+\cos^2\theta}}{1 + A_e A_\tau \cdot \frac{2\cos\theta}{1+\cos^2\theta}}. \quad (15)$$

In the previous section, by taking the mean value, the tau coupling,  $A_\tau$  has been isolated. By taking now the forward-backward asymmetry, the electron coupling,  $A_e$ , is isolated. The results are shown in fig. 11. The sensitivity of the method largely depends on the range of  $\cos\theta$  available for the analysis. In this respect, ALEPH has the advantage of being able to reach  $|\cos\theta| = 0.9$  compared to 0.7 for the other experiments. The error is still mainly statistical, since most systematic effects cancel out when computing the forward-backward asymmetry.

Fig. 11 shows the result from the asymmetry, from the mean, and the average between them, which assumes lepton flavour universality. For comparison, the recent, very precise, measurement of the left-right polarization asymmetry,  $A_{LR}$ , by the SLD collaboration is also given. This variable also measures the electron coupling,  $A_e$ . At the moment, the two determinations of  $A_e$  disagree at the level of three standard deviations. It is rather difficult to come up with a physical explanation for the difference, which should rather be assigned to statistical fluctuations or experimental problems.

### 4.4 Heavy Flavour Forward-Backward Asymmetries

The forward-backward asymmetries of quarks are very powerful in measuring the effective mixing angle. What is measured is

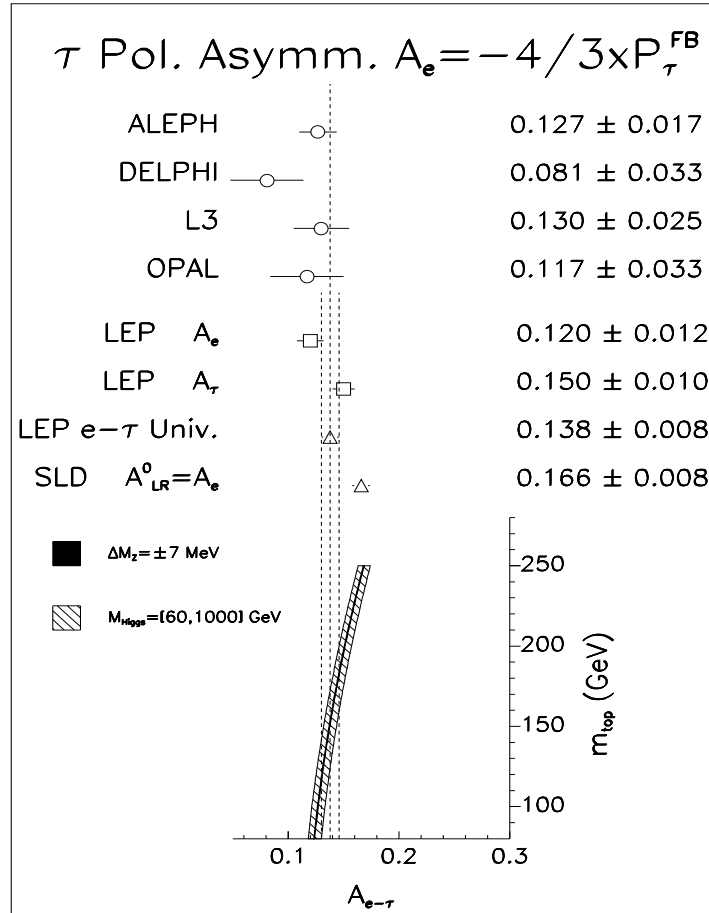
$$A_{FB}^{0,q} = \frac{3}{4} A_e A_q. \quad (16)$$

Since  $A_q$  is large ( $\sim 0.66, 0.93$  for u- and d-type quarks, respectively) and depends weakly on  $\sin^2\theta_W^{eff}$ , the asymmetry is quite large and mainly sensitive to the  $\sin^2\theta_W^{eff}$  dependence of  $A_e$ . The main difficulty measuring the forward-backward asymmetry for quark final states is to assign a positive or negative charge to a jet and to identify the flavour.

In the case of b quarks, the distinctive features that were mentioned in section 3 can be used to identify the b events. Two methods are used to get the charge of the quark. In the more traditional method, the charge of a high  $p$ , high  $p_t$  lepton from semileptonic decays which identify the b events is also used to extract the charge of the parent quark. In another, newer, method, the lifetime information in one hemisphere is used to tag the event while the weighted mean charge in the other hemisphere measures the quark charge. The two methods lead to samples almost completely statistically independent. The systematical errors differ as well: in the first method, the knowledge of the lepton purities and of the semi-leptonic



Figure 11: The tau polarization forward-backward asymmetry measured by the four experiments together with the mean and the MSM prediction as a function of the top quark mass. Also the SLD measurement of the left-right asymmetry is shown. The error definitions are those of fig. 1.

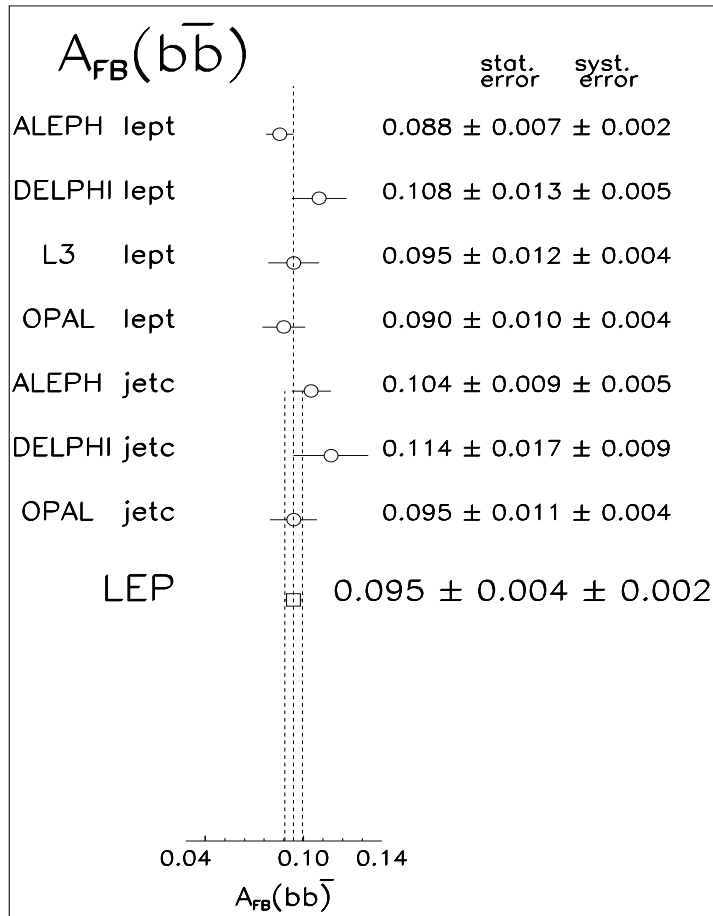


branching ratios is crucial; in the second, the charm background in the b sample is the main worry.

Results using both methods are shown in fig. 12 for b quarks. In fig. 13 measurements of  $A_{FB}$  for c quarks are shown. The precision of this latter measurement is considerably worse due to the lower efficiencies and purities for c quark separation. The results given in fig. 12 and 13 have to be corrected for QED, QCD and energy effects to obtain  $A_{FB}^{0,q}$  as appearing in eq. 16. After the corrections, the results are

$$\begin{aligned}
 A_{FB}^{0,b} &= 0.097 \pm 0.004 \pm 0.002 \\
 A_{FB}^{0,c} &= 0.072 \pm 0.008 \pm 0.007
 \end{aligned}
 \tag{17}$$

Figure 12: The b quark forward-backward asymmetry measured by the four experiments together with the mean. The error definitions are those of fig. 1.



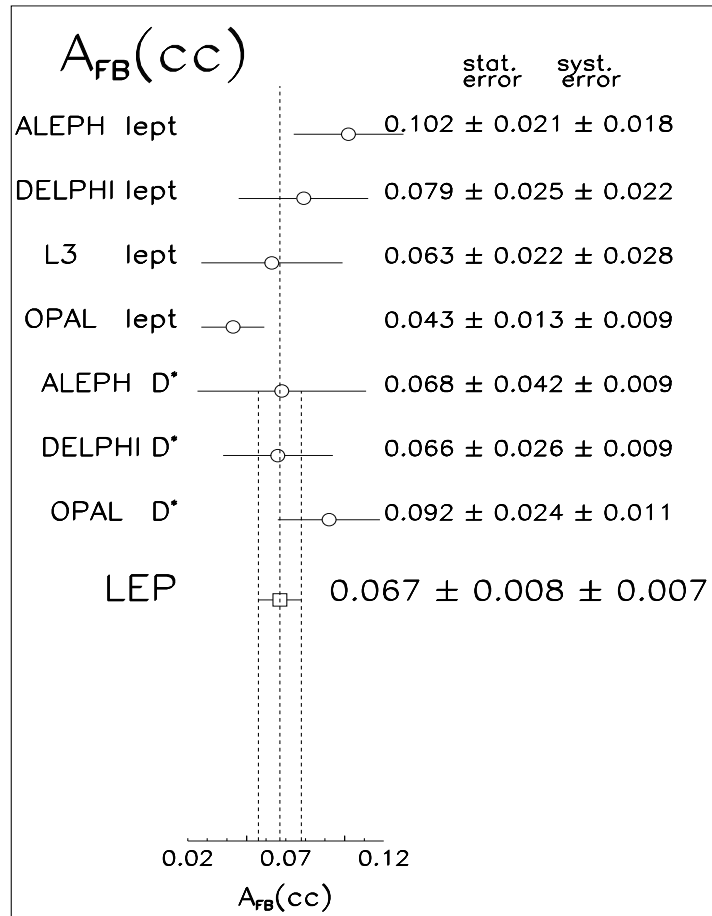
where the first error is statistical and the second systematic.

#### 4.5 Quark Forward-Backward Asymmetry (all flavours)

Using the same idea as in the vertex-tag method for  $A_{FB}^b$ , one can try to get the average quark charge via a momentum-weighted mean of hadron charges. This way, the forward-backward asymmetry for all flavours can be extracted. The precise definition of the observable is the following:

$$\langle Q_{FB} \rangle = \left\langle \frac{\sum_F q_i p_{iL}^k}{\sum_F p_{iL}^k} - \frac{\sum_B q_i p_{iL}^k}{\sum_B p_{iL}^k} \right\rangle = c A_e \sum_q \delta_q A_q \frac{\Gamma_q}{\Gamma_h} \quad (18)$$

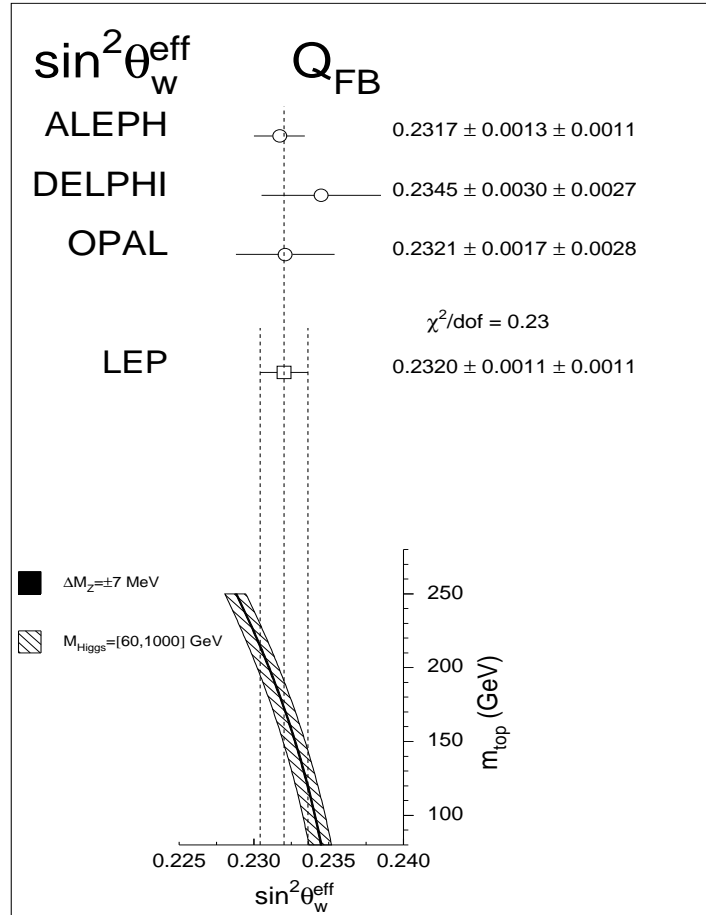
Figure 13: The c quark forward-backward asymmetry measured by the four experiments together with the mean. The error definitions are those of fig. 1.



where  $c$  is a normalization constant,  $p_L$  is the longitudinal momentum along the thrust axis and  $\kappa$  an arbitrary number that defines the weight. The quantity  $\delta_q$  is called the charge separation and measures the difference between the two hemisphere charges for a given flavour. This is the ingredient which is more difficult to obtain, the one which determines the size of the systematic error. For b quarks, it can be obtained from data, using semileptonic events, for instance. For the rest, it is obtained from Monte Carlo, although work is in progress to get the c quark contribution also from data.

The measurements from three of the four collaborations are shown in fig. 14. The resulting uncertainty in  $\sin^2 \theta_W^{eff}$  is competitive with the other measurements, with the caveat of its

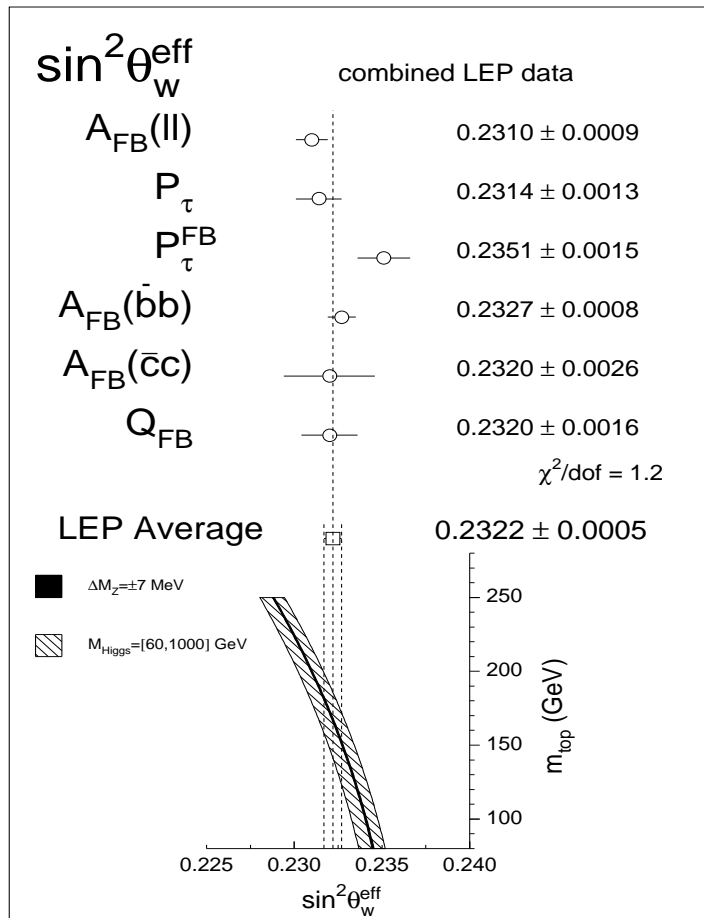
Figure 14: The effective weak mixing angle obtained from the quark forward-backward asymmetry measured by three experiments together with the mean and the MSM prediction as a function of the top quark mass. The error definitions are those of fig. 1.



heavy reliance on Monte Carlo, which should be reduced in the future.

Figure 15 shows all the values of  $\sin^2 \theta_W^{\text{eff}}$  obtained from the asymmetry measurements at LEP presented in the previous sections. The results agree well among themselves and the mean value provides a very precise determination of the effective weak mixing angle, which is very sensitive to the top quark mass.

Figure 15: LEP averages for  $\sin^2 \theta_W^{eff}$  obtained from the different asymmetry observables discussed in the text, together with the mean and the MSM prediction as a function of the top quark mass.



## 5 Standard Model Fits

The results presented in the previous sections can be interpreted in the context of the Minimal Standard Model. As mentioned in the introduction, the comparison of theory and experiment can lead to an indirect determination of the top quark mass. The comparison is made through a fit of the following LEP quantities:  $M_Z$ ,  $\Gamma_Z$ ,  $R_l$ ,  $\sigma_h^0$ ,  $R_b$  and  $\sin^2 \theta_W^{eff}$  from all asymmetries, and (optionally) non-LEP information:

- The ratio of the W and Z masses as measured by the UA2 Collaboration:  $M_W/M_Z = 0.8133 \pm 0.0041$  [9].

- The direct measurement of the W mass at the Tevatron collider:  $M_W = (79.89 \pm 0.28)$  GeV [10].
- The determination of the ratio of the W and Z masses from neutrino scattering experiments:  $1 - M_W^2/M_Z^2 = 0.2256 \pm 0.0047$  [11].

The parameters left free in the fit are the top quark mass and the value of  $\alpha_s$ . The Higgs boson mass is fixed to 300 GeV and, afterwards, varied in the range between 60 and 1000 GeV. The results of the fit using only LEP data are the following:

$$\begin{aligned} m_t &= (165^{+13+18}_{-14-19}) \text{ GeV} \quad \text{and} \\ \alpha_s(M_Z^2) &= 0.125 \pm 0.005 \pm 0.002 , \end{aligned} \tag{19}$$

with  $\chi^2/d.o.f. = 13.6/9$ , where the second error in each parameter reflects the uncertainty due to the Higgs mass. After including the non-LEP data, the result becomes

$$\begin{aligned} m_t &= (166^{+12+17}_{-13-19}) \text{ GeV} \quad \text{and} \\ \alpha_s(M_Z^2) &= 0.125 \pm 0.005 \pm 0.002 , \end{aligned} \tag{20}$$

with  $\chi^2/d.o.f. = 13.7/12$ . If the SLD measurement of the left-right asymmetry is included in the fit, the central value for the top quark mass gets higher, 174 GeV, and the quality of the fit degrades substantially,  $\chi^2/d.o.f. = 23.3/13$ .

As can be seen from the previous results, given the current precision of LEP data, non-LEP data does not add very much information. The quality of the fit is good, but there is a big contribution to the  $\chi^2$  from the branching ratio to b quarks, which, as mentioned in section 3, prefers a very low top quark mass.

The  $\chi^2$  of the fit including LEP and non-LEP data increases from 12.9 to 15.5 when the Higgs mass is moved from 60 to 1000 GeV. This variation is too small to draw any conclusion about the value of the Higgs mass based on the current data. A precise, direct determination of the top quark mass at FNAL would certainly help in this respect.

## 6 Summary

The data taken during 1993 at LEP have been used to measure the electroweak parameters related to the Z boson. The results agree with the Minimal Standard Model predictions. A hint of a discrepancy can be seen in the Z branching fraction to b quarks, but more data and further study of the systematic errors are needed before a conclusion can be reached.

Within the MSM, the top quark mass has been determined indirectly with a  $\sim 20$  GeV accuracy. At present, there is no useful sensitivity to the Higgs boson mass.

## Acknowledgements

I would like to thank the four LEP collaborations for letting me use their unpublished data. I am very grateful to M. Martinez and M. Pepe-Altarelli, who performed the fits leading to the results presented here and helped me with the figures, and to R. Jacobsen, for his help in the machine-related topics. I want to express my sincere gratitude to Prof. S. Yamada and his team for the excellent organization of the symposium as well as for the very warm hospitality dispensed to all of us.

## References

- [1] The LEP Collaborations ALEPH, DELPHI, L3, OPAL and The LEP Electroweak Working Group, CERN-PPE/93-157.
- [2] M. Martinez, L. Garrido, R. Miquel, J. L. Harton, R. Tanaka, Z. Phys. C49 (1991) 645.
- [3] D. Bardin et al., Z. Phys. C44 (1989) 493; Nucl. Phys. B351 (1991) 1; Phys. Lett. B255 (1991) 290; CERN-TH 6443/92.
- [4] The Working Group on LEP Energy, private communication.
- [5] L. Arnaudon et al., The Working Group on LEP Energy and The LEP Collaborations ALEPH, DELPHI, L3, OPAL, Phys. Lett. B307 (1993) 187.
- [6] T. Hebbeker, M. Martinez, G. Passarino, G. Quast, CERN-PPE/94-44.
- [7] S. Jadach et al., Comp. Phys. Comm. 70 (1992) 305, and private communication.
- [8] V. S. Fadin et al., JINR-E2-92-577.
- [9] J. Alitti et al., UA2 Coll., Phys. Lett. B241 (1990) 150.
- [10] F. Abe et al., CDF Coll., Phys. Rev. Lett. 65 (1990) 2243.  
Y. Ducros, in "Results and Perspectives in Particle Physics", La Thuile, March 6–12, 1994.
- [11] C. G. Arroyo et al., CCFR Coll., Columbia University preprint NEVIS R#1498, November 1993.  
H. Abramowicz et al., CDHS Coll., Phys. Rev. Lett. 57 (1986) 298; A. Blondel et al., Z. Phys. C45 (1990) 361.  
J. V. Allaby et al., CHARM Coll., Phys. Lett. B177 (1986) 446; Z. Phys. C36 (1987) 611.